Supplement of Atmos. Meas. Tech., 19, 5989–6014, 2026
https://doi.org/10.5194/amt-19-5989-2026-supplement

Atmospheric Measurement Techniques
Open Access
EGU

Supplement of

A new balloon-borne system for measuring the vertical variability of aerosol optical properties using low-cost sensors

Michalina Broda et al.

Correspondence to: Michalina Broda (michalina.broda@fuw.edu.pl)

S1 SPS30 lab testing and calibration

Figure S1 shows the rotational speed of the SPS30 internal fan measured in a laboratory vacuum chamber over the pressure range 1000–50 hPa, as described in Sect. 3 of the main manuscript.

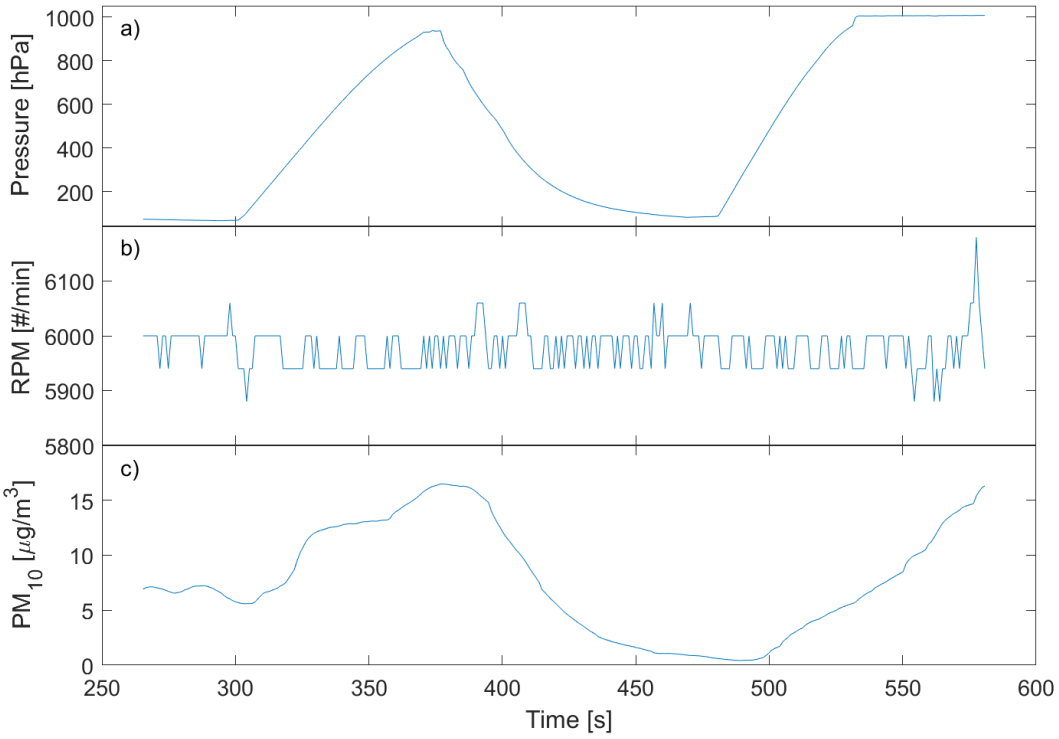

Figure S1. Temporal variability of (a) air pressure [hPa], (b) fan rotational speed (RPM) in SPS30, and (c) PM_{10} mass concentration during measurements in the vacuum chamber.

S2 Aerosol scattering coefficient simulations

Figure S2 shows the relationship between the aerosol scattering coefficient and PM_{10} derived from Lorenz–Mie simulations, supporting the functional form of Eq. (1) in the main manuscript.

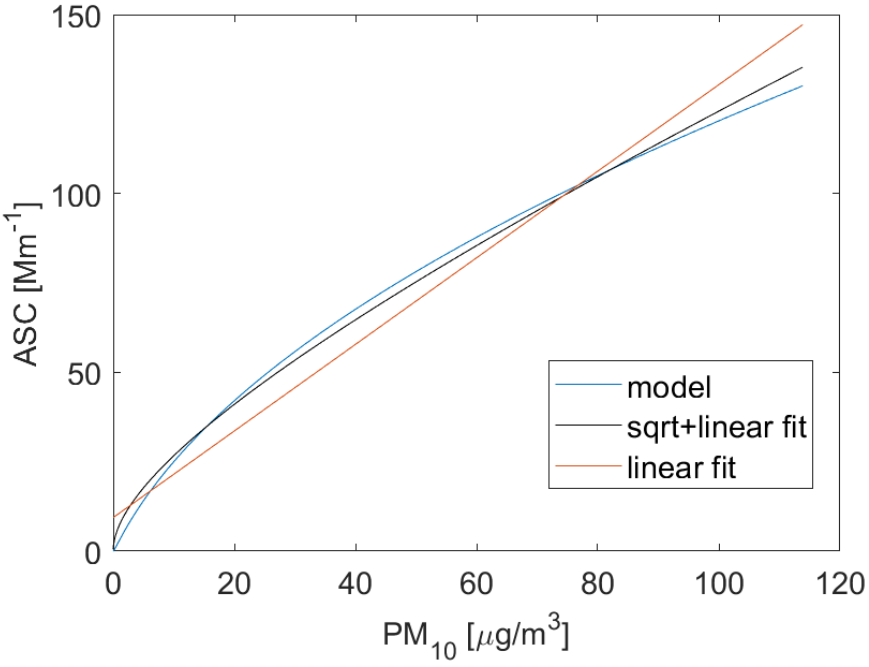

Figure S2. Aerosol scattering coefficient [Mm^{-1}] as a function of PM_{10} [$\mu g\ m^{-3}$] (blue line), derived from Lorenz–Mie simulations for spherical particles with a refractive index of (1.50 + 0.004i), representative of brown carbon from biomass burning (Sumlin et al., 2018). Calculations were performed assuming a log-normal size distribution with a fixed geometric standard deviation of 2.0 and a mode radius varying from 0.01 to 0.25 μm. The green line denotes a linear fit ($ASC = c \cdot PM_{10}$), while the black line represents a combined square-root and linear fit ($ASC = a \cdot PM_{10}^{1/2} + b \cdot PM_{10}$).

S3 Terrain elevation along the AeroSonde trajectories

Figure S3 shows the terrain elevation beneath the AeroSonde along the five soundings, used to assess the influence of orography on the observed aerosol layering (Sect. 2.3.2 of the main manuscript).

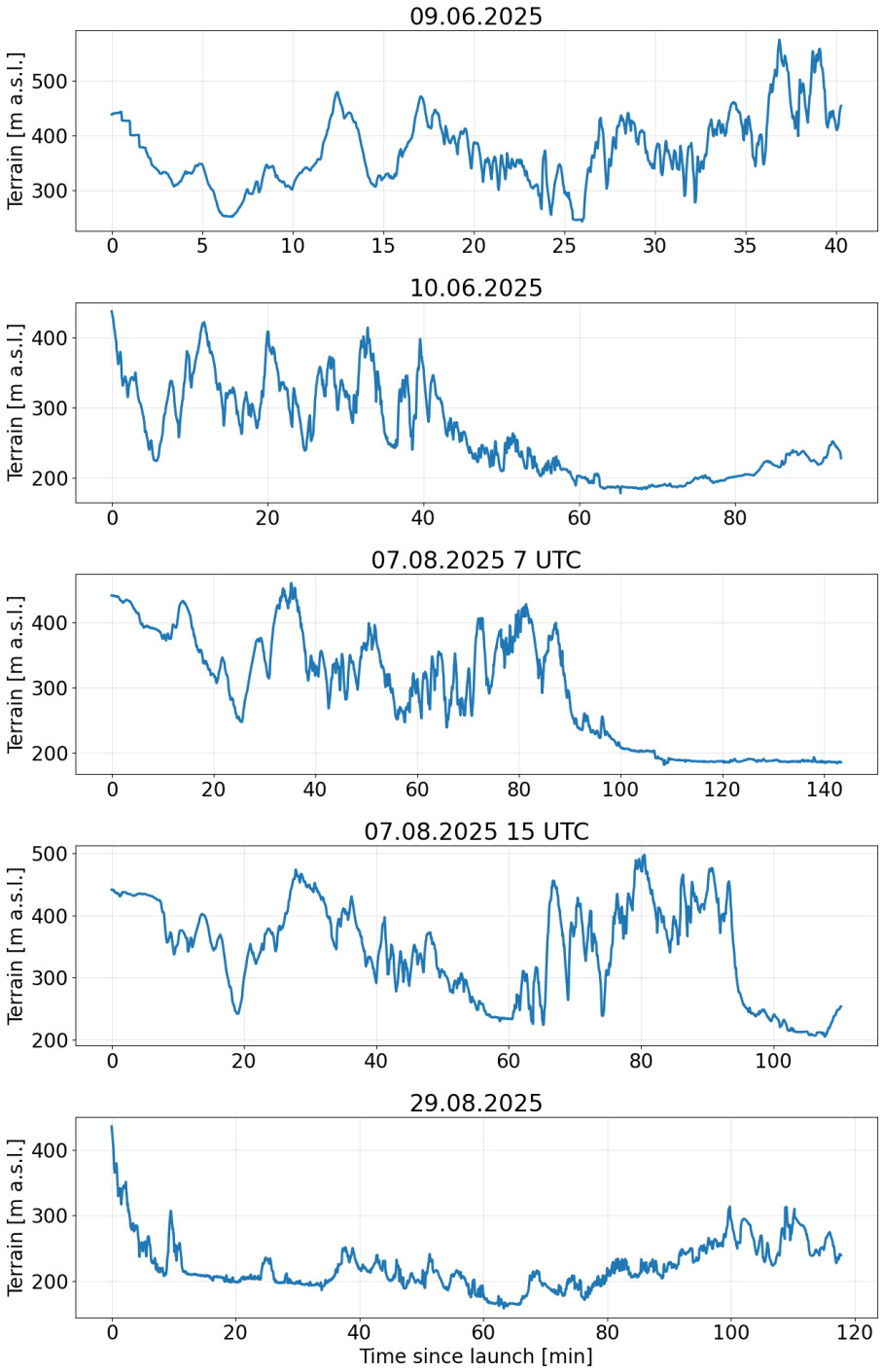

Figure S3. Terrain elevation beneath the AeroSonde as a function of time since launch, for the five soundings analysed in this study. Elevation was extracted along the GPS track recorded by the AeroSonde.

S4 Columnar aerosol properties during the AeroSonde ascents

Table S1 summarises the columnar aerosol properties observed at the Strzyżów site during the five AeroSonde ascents, together with the modelled contributions of smoke and mineral dust to the total aerosol optical depth. These values provide the atmospheric context for the case studies discussed in the main text and are the input to the AOD_{532} and SSA_{532} values compared with the AeroSonde retrievals there.

Table S1. Columnar aerosol properties at the SolarAOT station in Strzyżów during the five AeroSonde ascents. Aerosol optical depth at 500 nm (AOD_{500}) and the Ångström exponent between 440 and 870 nm ($AE_{440-870}$) are taken from the AERONET direct-sun product (level 1.5); single scattering albedo at 440 nm (SSA_{440}) and effective radius (R_{eff}) are taken from the AERONET almucantar inversion product (level 1.5). Times in parentheses (UTC) indicate the individual retrievals used, selected as those closest in time to each ascent. The last two columns give the fractional contributions of smoke (AOD_{smoke}/AOD) and mineral dust (AOD_{dust}/AOD) to the total AOD at 550 nm from the ICAP multi-model ensemble, taken at the closest available forecast time within ± 3 h of the measurement. Level 1.5 inversion products are not cloud-screened to level 2.0 standards; in addition, the AERONET quality criterion for SSA retrievals ($AOD_{440} > 0.4$) was not met on any of these days, so the SSA and R_{eff} values should be treated as indicative. N.A. denotes retrievals unavailable for a given time.

Date	**AERONET**				**ICAP**	
	AOD_{500}	**$AE_{440–870}$**	**SSA_{440}**	**R_{eff} [μm]**	**AOD_{smoke}/AOD**	**AOD_{dust}/AOD**
09 Jun 2025	0.45 (17:33)	1.47 (17:33)	0.974 (17:08)	0.249 (17:08)	0.47	0.06
10 Jun 2025	0.46 (12:18)	1.50 (12:18)	N.A.	N.A.	0.53	0.06
07 Aug 2025	0.27 (07:06)	1.67 (07:06)	0.953 (07:07)	0.221 (07:07)	0.61	0.02
07 Aug 2025	0.23 (15:25)	1.66 (15:25)	0.996 (12:40)	0.310 (12:40)	0.61	0.02
29 Aug 2025	0.28 (15:30)	0.40 (15:30)	0.927 (15:21)	0.734 (15:21)	0.11	0.58

S5 Biomass burning aerosol (case 1)

During the AeroSonde launches at 15:00 UTC, the maximum altitudes from which the signal was received were 19.3 km. The mean vertical resolution of the AeroSonde data was 5.4 ± 2.4 m. Due to the weak wind, the AeroSonde was within 1 km at 2 km, about 10 km at 5 km, and around 35 km at 10 km altitude. The wind profile measured by the meteorological sonde explains this horizontal displacement. Wind speeds remained below 7 ms^{-1} up to 4 km a.g.l. and increased only above this level, reaching less than 20 ms^{-1} at 10 km. Near the surface, the wind was from the southeast; however, already at around 1.5 km a.g.l. the flow shifted to a westerly direction, and above 7 km a southwesterly flow prevailed.

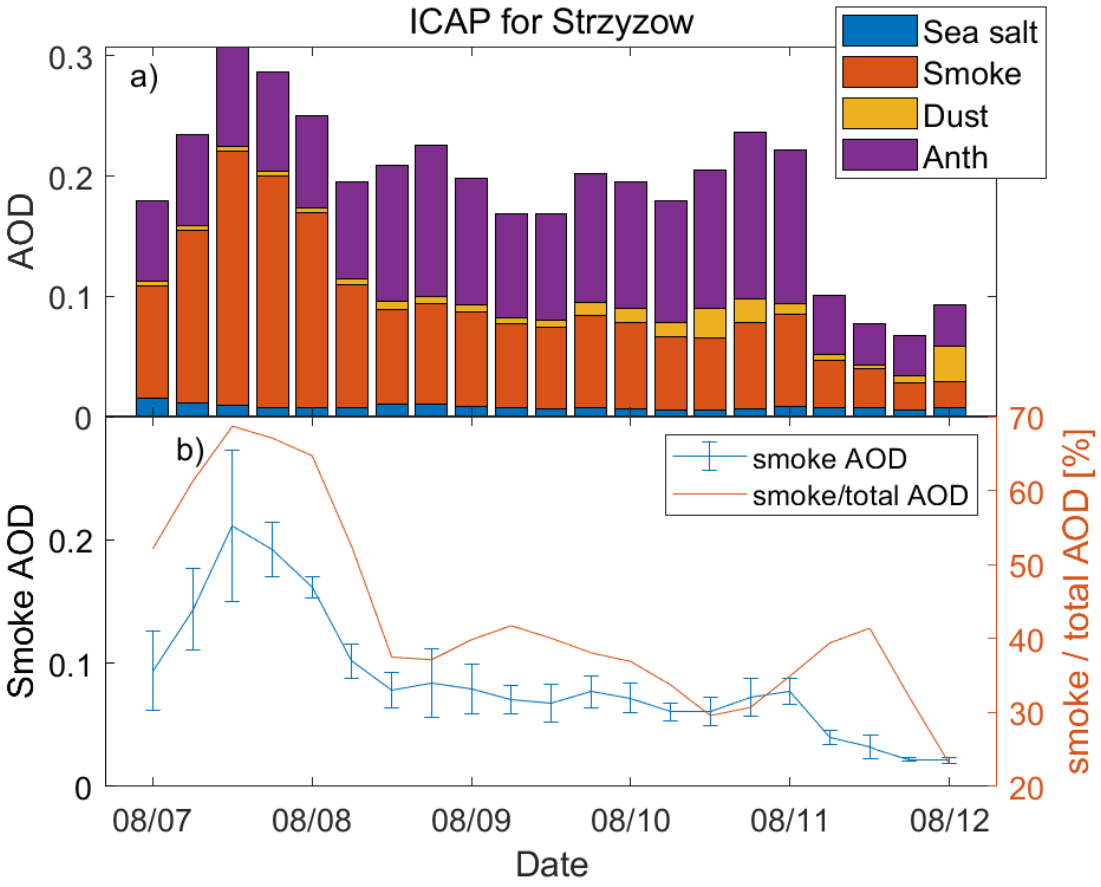

Figure S4. Total AOD with four categories distinguished (sea salt, smoke, dust, and anthropogenic) (a), and smoke AOD (b) at the Strzyżów site in the 7–12 August 2025 period (left y-axis), with the ratio of smoke to total AOD on the right y-axis. Values were retrieved from the ICAP model and are given at 550 nm.

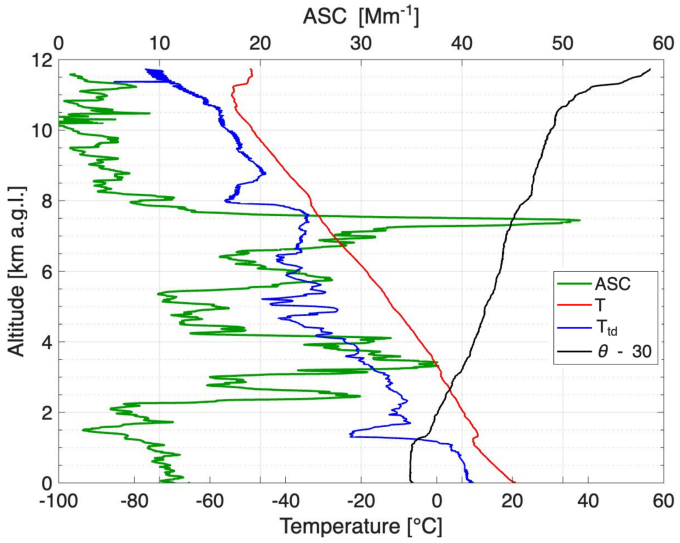

Figure S5. Vertical profiles of thermodynamic variables and aerosol scattering coefficient (ASC) obtained from the AeroSonde sounding on 7 August in the afternoon. The vertical axis represents height (km a.g.l.). Temperature is shown on the lower horizontal axis, while the ASC is shown on the upper horizontal axis (Mm^{-1}). The red line denotes the air temperature profile (T), the blue line represents the dew-point temperature (T_{td}), and the black line shows the potential temperature (θ), shifted by -30 °C for clarity. The green line corresponds to the vertical profile of the ASC.

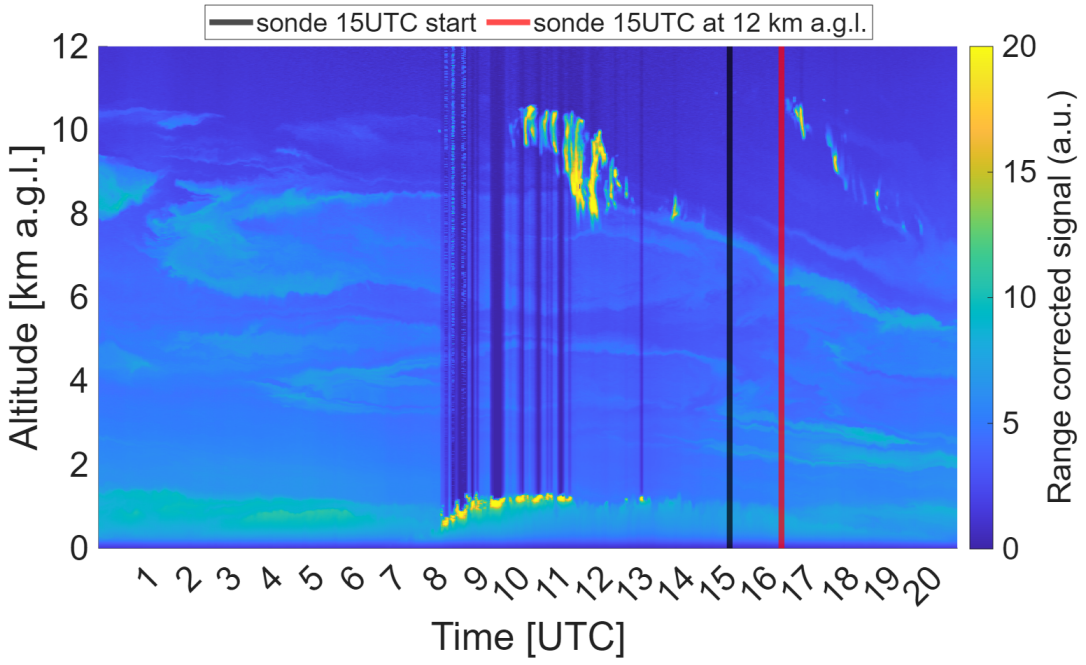

Figure S6. Lidar range corrected signal at 532 nm for 7 August 2025. The black line indicates the AeroSonde flight start, while the red line points to the time of reaching the 12 km a.g.l.

S6 Dust aerosol

During these measurements, the maximum altitude from which data were received reached 26.8 km after 2.5 hours of ascent. The mean vertical resolution of the AeroSonde data was 5.3 ± 2.1 m. At 2 km a.g.l., the AeroSonde was already located about 10 km from the station, at 5 km the distance increased to 28 km, and at 10 km it reached approximately 65 km from the station. Wind near ground level (500 m a.g.l.) was blowing from north with a speed of around 2.5 ms^{-1}. But at 1.5 km a.g.l. it started blowing from the southwest with a velocity minimum 15 ms^{-1}, which was up to 12 km, where it reached 25 ms^{-1}.

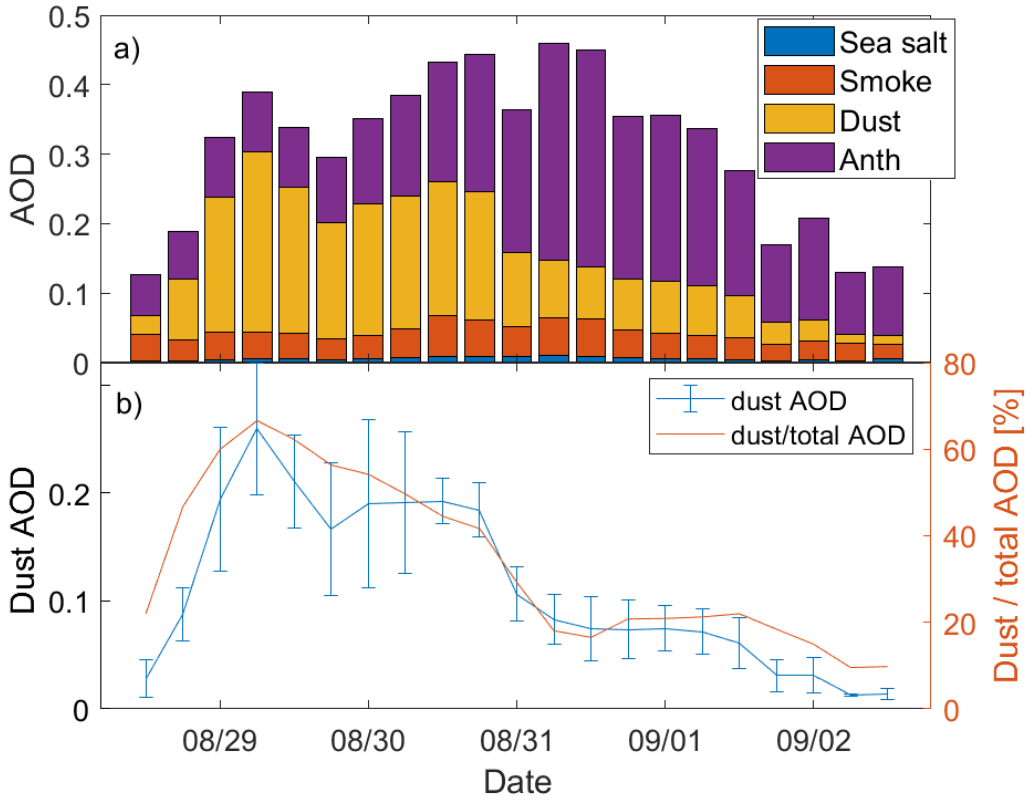

Figure S7. Total AOD with four categories distinguished (sea salt, smoke, dust, and anthropogenic) (a), and dust AOD (b) at the Strzyżów site in the 28 August–3 September 2025 period (left y-axis), with the ratio of dust to total AOD on the right y-axis. Values were retrieved from the ICAP model and are given at 550 nm.

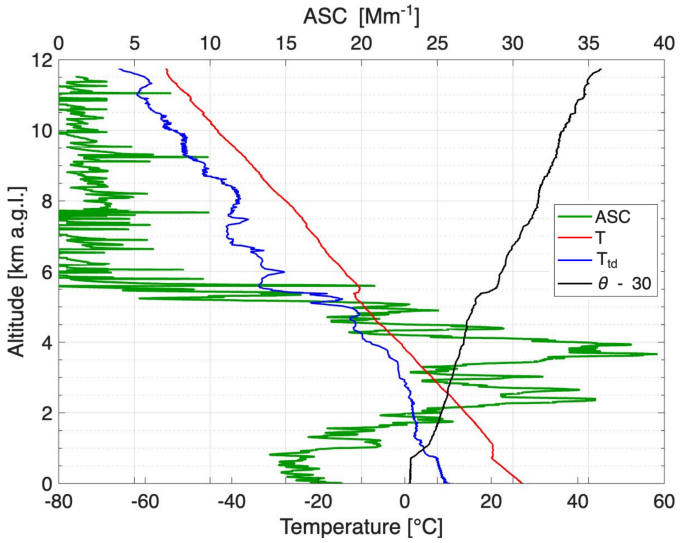

Figure S8. Vertical profiles of thermodynamic variables and aerosol scattering coefficient (ASC) obtained from the AeroSonde sounding on 29 August. The notation follows Fig. S5.

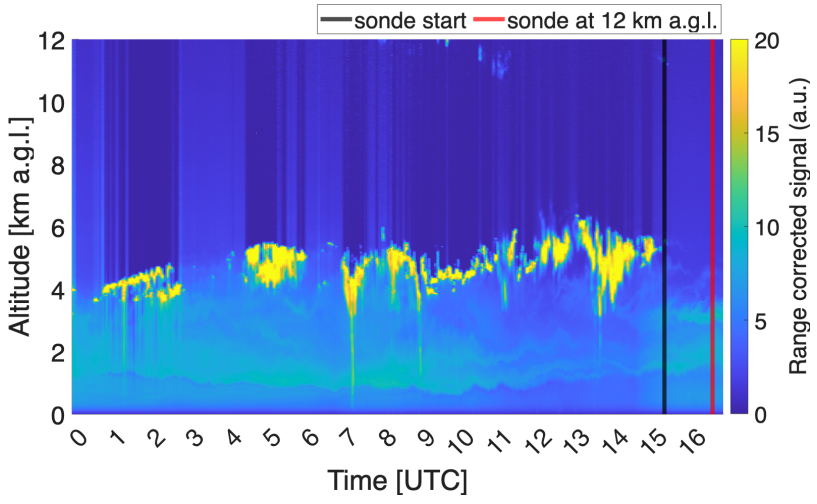

Figure S9. Lidar range corrected signal for 29 August 2025. The black line indicates the AeroSonde flight start, while the red line points to the time of reaching the 12 km a.g.l.

References

Sumlin, B., Heinson, Y., Shetty, N., Pandey, A., Pattison, R., Baker, S., Hao, W., and Chakrabarty, R.: UV–Vis–IR spectral complex refractive indices and optical properties of brown carbon aerosol from biomass burning, Journal of Quantitative Spectroscopy and Radiative Transfer, 206, 392–398, https://doi.org/https://doi.org/10.1016/j.jqsrt.2017.12.009, 2018.